Effective neoantigen vaccination correlates with cDC1-dependent generation of antigen-specific CX3CR1+CD8+ T cells in mice

Takayoshi Yamauchi[1,6], Toshifumi Hoki[1,6], Takaaki Oba[1,6], Kristopher Attwood[2], Xuefang Cao[3], and Fumito Ito,[1, 4, 5, *]

[1] Center for Immunotherapy, Roswell Park Comprehensive Cancer Center, Buffalo, NY, USA

[2] Department of Biostatistics and Bioinformatics, Roswell Park Comprehensive Cancer Center, Buffalo, NY 14263, USA

[3] Department of Microbiology and Immunology, University of Maryland School of Medicine, Baltimore MD, USA

[4] Department of Surgical Oncology, Roswell Park Comprehensive Cancer Center, Buffalo, NY, USA

[5] Department of Surgery, Jacobs School of Medicine and Biomedical Sciences, State University of New York at Buffalo, Buffalo, NY 14263, USA

[6] Co-first author

* Corresponding author

Please address all correspondence to F. Ito

Elm and Carlton Streets, Buffalo, NY 14263

Phone: 716-845-1300 FAX: 716-845-1595

Email: fumito.ito@roswellpark.org

Key words: neoantigen, vaccine, CX3CR1, Batf3, dendritic cells, cDC1, CD40, CD70, CD80, CD86, T cells

Grant support: This work was supported by Roswell Park Comprehensive Cancer Center and its National Cancer Institute (NCI) award, P30CA016056 involving the use of Roswell Park's Flow and Image Cytometry and Genomic Shared Resources. F.I was supported by Roswell Park Alliance Foundation and NIH/NCI K08CA197966. X.C. was supported by NIH/ R01HL135325. T.Y. was supported by Astellas Foundation for Research on Metabolic Disorders, and the Nakatomi Foundation. T.O. was supported by Uehara Memorial Foundation.

Running title: CX3CR1 as a circulating biomarker for vaccine therapy

Abstract

The use of tumor mutation-derived neoantigen represents a promising approach for cancer vaccines. Preclinical and early-phase human clinical studies have shown the successful induction of tumor neoepitope-directed responses; however, overall clinical efficacy of neoantigen vaccines has been limited. One major obstacle of this strategy is the lack of a reliable blood-based surrogate marker for clinical response. Here, we report a correlation between antitumor efficacy of neoantigen/toll-like receptor 3 (TLR3)/CD40 vaccination and the frequency of circulating antigen-specific $CD8^+$ T cells expressing CX3C chemokine receptor 1 (CX3CR1) in a preclinical model. Mechanistic studies using mixed bone marrow chimeras identified critical roles of CD40 and CD80/86, but not CD70 signaling in Batf3-dependent conventional type 1 dendritic cells (cDC1s) in antitumor efficacy of neoantigen vaccine and generation of neoantigen-specific $CX3CR1^+CD8^+$ T cells. Despite robust effector function *in vitro*; however, depletion of $CX3CR1^+$ $CD8^+$ T cells did not alter antitumor efficacy of neoantigen/TLR3/CD40 agonists vaccination, suggesting that CX3CR1 expression is purely a biomarker rather than functionally relevant to the established tumors. Taken together, our results underscore a critical role of cDC1s in neoantigen-based therapeutic vaccines, and the potential utility of CX3CR1 as a circulating surrogate marker for vaccine efficacy in clinical studies.

57 # Introduction

58 Despite objective therapeutic benefit seen in several clinical trials, the overall clinical
59 success of the peptide-based vaccines has thus far been limited (1, 2). This is due, at least in part,
60 to the low immunogenicity of self-antigens, the incomplete understanding of immunological
61 mechanisms underlying effective priming of tumor-specific T cells, and the lack of a reliable
62 biomarker for clinical response. Somatically mutated genes within tumors can generate
63 neoantigens, which create *de novo* epitopes for T cells (3). Since neoantigens have not undergone
64 central thymic selection, they can be deemed as highly immunogenic tumor-specific antigens (3).
65 Recent advances of neoantigen identification by massive parallel sequencing and computational
66 prediction of neo-epitopes have demonstrated that individualized mutanome-based vaccinations
67 are promising (4-9).

68 Intratumoral infiltration of $CD8^+$ T cells is an independent prognostic factor for survival
69 of patients with various cancer types (10, 11). In contrast, increases in peripheral blood (PB)
70 tumor-associated antigen-specific T cells following immunization do not necessarily translate
71 into antitumor effects (12). Analysis of T-cell infiltrates in serially obtained tumor samples
72 would be ideal to evaluate response to vaccine therapy; however, it is invasive and especially
73 challenging for visceral tumors. Identification of circulating biomarkers that correlate with
74 effectiveness of vaccination and clinical outcome of patients would markedly improve current
75 treatment regimens.

76 The chemokine receptor, CX3CR1, was recently identified as a marker of effector T-cell
77 differentiation (13, 14). Unlike other proliferation, co-stimulatory and co-inhibitory molecules
78 such as Ki67, ICOS, PD-1 and CTLA-4 that are only transiently upregulated on T cells after
79 activation, CX3CR1 is stably expressed on virus- and tumor-specific $CD8^+$ T cells upon

80 differentiation via unidirectional differentiation from the CX3CR1- subset during the effector
81 phase (13-15). Furthermore, our study and others have shown that CD8+ T cells expressing
82 high levels of CX3CR1 exhibit decreased expression of L-selectin (CD62L) and CXCR3 (13-
83 15), trafficking receptors necessary for entry across lymphoid organ high endothelial venules
84 (HEV) and the tumor microvasculature (16, 17), respectively, and become more prevalent in
85 PB at the end of the effector phase (14, 15), suggesting a potential advantage as a circulating T-
86 cell biomarker. These observations prompted us to hypothesize that effective vaccination
87 would be associated with the increased frequency of antigen-specific CX3CR1+CD8+ T cells in
88 the periphery.

89 Here, we used a syngeneic mouse model of colon adenocarcinoma with the neo-epitope
90 presented in major histocompatibility complex (MHC) class I H-2Db molecules (18), and
91 investigated the relationship between antitumor efficacy of neoantigen vaccination and the
92 frequency of neoantigen-specific CX3CR1+CD8+ T cells. Our results indicate that generation of
93 circulating neoantigen-specific CX3CR1+CD8+ T cells correlates with successful vaccination
94 with mutated peptide and toll-like receptor 3 (TLR3)/CD40 agonists. Mechanisms underlying the
95 generation of CX3CR1+CD8+ T cells were examined using knockout and bone marrow chimeric
96 mice. *In vivo* antitumor reactivity of CX3CR1+ subsets was evaluated in mice genetically
97 modified to express diphtheria toxin receptors (DTR) on CX3CR1+ T cells.

98

99

100 # Results

101 **Vaccination with neoantigen and TLR3/CD40 agonists elicits potent antigen-specific**
102 **antitumor efficacy.**

103 To examine the relationship between antitumor efficacy of neoantigen vaccination and
104 the generation of neoantigen-specific CX3CR1+CD8+ T cells, we sought to validate a preclinical
105 model of neoantigen vaccination using MC38 colon adenocarcinoma cells that harbor a single-
106 epitope mutation within the Adpgk protein (**Supplemental Figure 1**) (18). In this model, to
107 maximize the therapeutic efficacy of neoantigen vaccination with mutant Adpgk peptide
108 ($Adpgk_{Mut}$), dual TLR/CD40 stimulation was used as vaccine adjuvants **(Figure 1A**), which has
109 been known to synergistically activate DCs, augment CD8+ T cell expansion, and mediate potent
110 antitumor immunity in multiple preclinical models (19-22). Vaccination of $Adpgk_{Mut}$, but not
111 irrelevant AH1 peptide with agonistic anti-CD40 antibody (Ab), and TLR3 agonist, poly(I:C)
112 (referred to as $Adpgk_{Mut}$/TLR3/CD40 hereafter) markedly delayed the growth of established
113 MC38 tumors and improved survival **(Figure 1B**). Splenocytes and tumor-infiltrating cells from
114 MC38 tumor-bearing mice treated with $Adpgk_{Mut}$/TLR3/CD40 vaccination contained
115 substantially higher frequency of CD8+ T cells that could produce IFN-γ and TNF-α against
116 $Adpgk_{Mut}$ but not irrelevant AH1 antigen **(Figure 1C** and **Supplemental Figure 2**), suggesting
117 the generation of antigen-specific CD8+ T cells. These findings validate a preclinical model of
118 neoantigen vaccine-based therapy to investigate the role of CX3CR1 as a circulating surrogate
119 marker for vaccine efficacy.

120

121 **Effective neoantigen/TLR3/CD40 stimulations correlate with generation of antigen-specific**
122 **effector CX3CR1+CD8+ T cells.**

123 We examined whether effective neoantigen vaccination could generate CD8+ T cells
124 expressing CX3CR1, a marker of effector differentiation (13, 14). To this end, PB, spleen and
125 tumors were harvested 1 week after second Adpgk$_{Mut}$/TLR3/CD40 vaccination, and CX3CR1
126 expression was evaluated in CD8+ and neoantigen-specific CD8+ T cells using an Adpgk$_{Mut}$-
127 specific tetramer (Tet) (**Supplementary Figure 3**). Adpgk$_{Mut}$/TLR3/CD40 vaccination
128 substantially increased the frequency of CD8+ and Tet+CD8+ T cells expressing CX3CR1 in PB
129 and spleen while the frequency of the CX3CR1+ subset remained unchanged in tumors (**Figure**
130 **2A**).

131 Previous clinical studies showed that functional assessment of T cells such as IFN-γ
132 production and/or cytolytic activity was correlated with response in patients treated with peptide
133 vaccines (23-25). Therefore, we evaluated CX3CR1 expression of T cells expressing effector
134 cytokines, and found that the majority of CD8+ T cells producing effector cytokine against
135 Adpgk$_{Mut}$ were largely positive for CX3CR1 expression (**Supplementary Figure 4A**).
136 Accordingly, frequency of the CX3CR1+ subset in circulating Tet+CD8+ T cells correlated with
137 the frequency of CD8+ T cells secreting IFN-γ+ and TNF-α+ against Adpgk$_{Mut}$ antigen in spleen
138 (**Supplementary Figure 4B**).

139 Next, we assessed relationship between tumor volume and differentiation or expansion of
140 antigen-specific CD8+ T cells in PB from treated and untreated mice. There was a strong inverse
141 correlation between frequency of circulating CD8+ and Tet+CD8+ T cells expressing CX3CR1
142 and tumor volume while the frequency of total Tet+CD8+ T cells without CX3CR1 criteria had a
143 moderate inverse correlation with tumor volume **(Figure 2B**).

144 Phenotypical and functional evaluation of circulating Adpgk$_{Mut}$-specific CX3CR1- and
145 CX3CR1+ subsets revealed that the CX3CR1+ subset contained significantly more 4-1BB+, PD-

146 1+, KLRG+ and granzyme A (GZMA)+ populations (**Figure 2C**), suggesting recently-activated
147 effector T cells. However, CX3CR1+CD8+ T cells exhibited decreased expression of trafficking
148 molecules, CD62L and CXCR3, involved in T-cell access into lymphoid tissues and tumor
149 microenvironment (TME), respectively (16, 17), in line with the higher frequency of the
150 CX3CR1+ subset in PB in treated mice (**Figure 2A**).
151
152
153 **CD40 signaling is required for antitumor efficacy of neoantigen/TLR3/CD40 agonists and**
154 **generation of antigen-specific CX3CR1+CD8+ T cells.**
155 Neoantigen vaccination with a TLR3 agonist increases antigen-specific tumor-infiltrating
156 lymphocytes in a preclinical model (26) and patients (4, 5). CD40 signaling drives robust DC
157 activation to generate cytotoxic CD8+ T cells (27-29), and synergizes with the TLR3 ligand in
158 inducing an expansion of peptide or DC vaccine-primed and adoptively transferred antigen-
159 specific CD8+ T cells (19, 22, 30, 31). To delineate a role of CD40 signaling in the context of
160 neoantigen vaccination, we examined antitumor efficacy of Adpgk$_{Mut}$/TLR3/CD40 vaccination
161 and generation of Adpgk$_{Mut}$-specific CX3CR1+CD8+ T cells using CD40-/- mice. Antitumor
162 efficacy of Adpgk$_{Mut}$/TLR3/CD40 vaccination was abrogated in CD40-/- mice (**Figure 3A**). The
163 lack of increase in the frequency of Adpgk$_{Mut}$-specific CX3CR1+CD8+ T cells in CD40-/- mice
164 denoted the requirement of CD40-CD40 ligand pathway in this process (**Figure 3B**), in line with
165 recent studies showing that CD4+ T-cell help or agonistic anti-CD40 Ab facilitates generation of
166 CX3CR1+CD8+ T cells (32, 33).
167

168 **Critical roles of CD40 signaling in cDC1s for antitumor efficacy of neoantigen/TLR3/CD40**
169 **agonists vaccination and generation of antigen-specific CX3CR1+CD8+ T cells.**

170 Batf3-dependent conventional type 1 dendritic cells (cDC1s) specialize in cross-
171 presentation of exogenous antigens on MHC class I molecules, and play a key role in antitumor
172 immunity and response to immunotherapy (26, 34-39). To assess whether cDC1s are necessary
173 for driving the formation of CX3CR1+CD8+ T cells, we employed mice deficient of Batf3
174 transcription factor, which is required for the maturation of cDC1s (40). No therapeutic efficacy
175 of AdpgkMut/TLR3/CD40 vaccination was observed in Batf3-/- mice (**Figure 4A**) along with a
176 significant reduction of CX3CR1+Tet+CD8+ T cells (**Figure 4B**), suggesting the requirement of
177 cDC1s for generation of antigen-specific CX3CR1+CD8+ T cells.

178 cDC1s express high levels of TLR3, and TLR3 agonist Poly-ICLC has been used in
179 personalized neoantigen vaccine trials with vaccine-related objective responses (5-7). However,
180 the role of CD40 signaling in cDC1s in vaccine-based immunotherapy remains elusive. To
181 address a direct role of CD40 signaling in cDC1 lineage for CX3CR1+CD8+ T cell development,
182 we generated CD40-/-/Batf3-/- or wild type (WT)/Batf3-/- mixed bone marrow chimeras into
183 irradiated C57BL/6 WT mice. CD40-/-/Batf3-/- bone marrow transplanted recipient mice (CD40-/-
184 plus Batf3-/- mixed bone marrow chimeras) lack CD40 expression only in Batf3-dependent bone
185 marrow-derived cells while WT/Batf3-/- bone marrow transplanted recipient mice have an intact
186 CD40 signaling. In CD40-/- plus Batf3-/- mixed bone marrow chimeras, CX3CR1+CD8+ T-cell
187 responses remained minimal compared to WT plus Batf3-/- mixed bone marrow chimeras,
188 indicating that CD40 expression on cDC1s is pivotal for the CX3CR1+CD8+ T-cell induction
189 (**Figure 4C**). In line with these results, mice reconstituted with CD40-/- plus Batf3-/- mixed bone

190 marrow chimeras had substantially decreased antitumor efficacy of Adpgk$_{Mut}$/TLR3/CD40
191 vaccination compared to mice with WT plus Batf3$^{-/-}$ mixed bone marrow chimeras (**Figure 4D**).
192
193 **Non-redundant requirement of CD80/86 but not CD70 signaling in cDC1s for antitumor**
194 **efficacy of neoantigen/TLR3/CD40 agonists vaccination and generation of antigen-specific**
195 **CX3CR1^{+}CD8^{+} T cells.**
196 In addition to CD40, both CD70 and CD80/86 have been reported to play roles in DC-
197 mediated T cell activation and persistence (41); however, the role of these molecules on cDC1s
198 for T-cell differentiation remains elusive. Therefore, the requirements of CD70 and CD80/86
199 signaling in cDC1s were assessed in mixed bone marrow chimeric mice of CD70$^{-/-}$ plus Batf3$^{-/-}$
200 and CD80/86$^{-/-}$ plus Batf3$^{-/-}$. There was no difference in the frequency of Adpgk$_{Mut}$-specific
201 CX3CR1^{+}CD8^{+} T cells between WT plus Batf3$^{-/-}$ and CD70$^{-/-}$ plus Batf3$^{-/-}$ mixed bone marrow
202 chimeras (**Figure 5A**) with similar tumor control (**Figure 5B**), suggesting a redundant role of
203 CD70 signaling in cDC1s. In sharp contrast, generation of Adpgk$_{Mut}$-specific CX3CR1^{+}CD8^{+} T
204 cells (**Figure 5C**) and antitumor efficacy of Adpgk$_{Mut}$/TLR3/CD40 vaccination (**Figure 5D**)
205 were abrogated in the CD80/86$^{-/-}$ plus Batf3$^{-/-}$ compared to the control WT plus Batf3$^{-/-}$ mixed
206 bone marrow chimeras. Thus, the CD80/86-CD28 pathway in cDC1s plays crucial roles in
207 mediating antitumor efficacy and generating antigen-specific effector CX3CR1^{+}CD8^{+} T cells in
208 the context of neoantigen vaccination. Taken together, effective neoantigen/TLR3/CD40 agonist
209 vaccination correlates with generation and frequency of circulating antigen-specific
210 CX3CR1^{+}CD8^{+} T cells mediated by CD40 and CD80/86 signaling in cDC1s.
211

212 ***In vivo* antitumor efficacy of antigen-specific CX3CR1+CD8+ T cells elicited by**
213 **neoantigen/TLR3/CD40 agonist vaccination.**

214 Previous preclinical studies using CX3CR1-/- mice or CX3CR1 inhibitor suggested a
215 significant role of the CX3CR1/CX3CL1 axis in T cell/NK-cell mediated antitumor immunity
216 (32, 42-45). However, CX3CR1 is expressed not only on T and NK cells, but also on
217 monocytes, DCs, monocytic myeloid-derived suppressor cells (M-MDSCs) and tumor-
218 associated macrophages (TAMs) (46, 47), and antitumor efficacy of CX3CR1+CD8+ T cells
219 against established tumors remains elusive. Recently, we have reported negligible antitumor
220 efficacy of CX3CR1hi CD8+ T cells using a mouse model where tumor antigen-specific
221 CX3CR1hi CD8+ T cells can be selectively depleted *in vivo* with diphtheria toxin (DT) (15).
222 Furthermore, adoptive transfer of CX3CR1+CD8+ T cells did not affect tumor growth nor
223 survival while the CX3CR1- subset displayed potent antitumor efficacy (15).

224 To elucidate antitumor efficacy of CX3CR1+CD8+ T cells elicited by
225 neoantigen/TLR3/CD40 agonists vaccination, we crossed CD2-Cre mice (48) with CX3CR1-
226 DTR mice (49), and generated *Cd2-cre/Cx3cr1+/DTR* mice. Expression of *Cd2-cre* excises the
227 *loxP*-floxed stop cassette upstream of the DTR-coding region, allowing for DTR expression
228 and CX3CR1+CD8+ T cells can be depleted upon administration of DT, with no effect on
229 CX3CR1-CD8+ T cells (**Figure 6A, B**). MC38 tumor-bearing *Cd2-cre/Cx3cr1+/DTR* mice were
230 treated with AdpgkMut/TLR3/CD40 vaccination, and received phosphate buffer saline (PBS) or
231 DT injections every day starting 1 day before vaccination (**Figure 6B**). We found that
232 depletion of CX3CR1+CD8+ T cells did not alter antitumor efficacy of neoantigen vaccination
233 (**Figure 6C**), in line with our recent study using a mouse model of adoptive T-cell therapy

234 (15), suggesting that CX3CR1+ CD8+ T cells might not be functionally relevant to the
235 established tumors while their frequency in PB correlates with response to the treatment.
236

237 # Discussion

238 In this study we have shown potent antitumor efficacy of neoantigen/TLR3/CD40
239 stimulations in a preclinical model, and identified a novel link between antitumor efficacy of
240 neoantigen vaccine and an increased frequency of circulating neoantigen-specific
241 CX3CR1+CD8+ T cells. Moreover, using mixed bone marrow chimeras from Batf3-/-, CD40-/-,
242 CD70-/-, and CD80/86-/- mice, we have revealed critical roles of CD40 and CD80/86 signaling in
243 cDC1s for generation of neoantigen-specific CX3CR1+CD8+ T cells and *in vivo* antitumor
244 efficacy of neoantigen/TLR3/CD40 agonists vaccination.

245 Engagement of CD40 on DCs induces costimulatory molecules on their surface,
246 promotes their cytokine production, facilitates the cross-presentation of antigen (50), and
247 synergistically augments expansion of both endogenous and adoptive transferred T cells (19, 20,
248 22, 30). Our data further demonstrated that cDC1s play a critical role in antitumor efficacy of
249 TLR3/CD40 stimulation. Although Poly-ICLC (TLR3 agonist) has been used in neoantigen
250 vaccine clinical studies (5, 6), these findings underscore the implication of agonistic anti-CD40
251 Ab in combination with Poly-ICLC for the maximal engagement of cDC1 in vaccine-based
252 therapy.

253 The molecular and cellular mechanisms underlying differentiation of CX3CR1- to
254 CX3CR1+CD8+ T cells remain elusive. Recent studies have indicated that CD4+ T-cell help or
255 agonistic anti-CD40 Ab facilitates generation of CX3CR1+CD8+ T cells (32, 33). Our results
256 further demonstrated the non-redundant requirement of CD40 signaling in cDC1s for the
257 generation of neoantigen-specific CX3CR1+CD8+ T cells. The observation that CD70 signaling
258 in cDC1s was dispensable for generation of the CX3CR1+ subset was unexpected given the
259 several lines of evidence suggesting that CD40 signaling relays the CD4+ T-cell help signal by

260 the induction of CD70 expression on DCs (51). However, not all molecules regulated by CD4+
261 T-cell help are mediated by CD27, and cytokine signaling may have contributed to the
262 generation of the CX3CR1+ subset (33). In support of this notion, IL-21 was found to modulate
263 T-cell differentiation and generation of CX3CR1+CD8+ T cells (32, 52). Additional mechanistic
264 studies are needed to further determine the signaling required for generation of the CX3CR1+
265 subset.

266 The lack of a reliable surrogate marker for clinical response remains the major limitation
267 of vaccine clinical trials (1, 2). Mere presence of vaccine-primed tumor-specific T cells might
268 not correlate with effective regression of the tumor, and cannot be used as a standalone
269 biomarker for vaccine efficacy (12). In our study, although frequency of PB antigen-specific
270 CD8+ T cells had a positive inverse correlation with tumor volume, differentiation of antigen-
271 specific CD8+ T cells defined by CX3CR1 expression had a markedly higher inverse
272 correlation with tumor volume. Furthermore, our findings of an increased frequency of
273 CX3CR1+CD8+ T cells that have the ability to produce IFN-γ, TNF-α and GZMA after
274 successful vaccination align with the evidence from previous clinical studies showing that
275 functional assessment of T cells such as IFN-γ production and/or cytolytic activity was
276 correlated with response in patients treated with peptide vaccines (23-25).

277 An increased frequency of the CX3CR1+ subset was identified not only in Tet+CD8+ T
278 cells, but also in total CD8+ T cells, which had a strong inverse correlation with tumor volume.
279 It remains unclear, however, whether this was due to an increased frequency of non-specific
280 CX3CR1+CD8+ T cells or an epitope-spreading phenomenon, the spread of the immune
281 response from one antigen to another antigen expressed in the same tissue (1, 2). Additional
282 studies are required to determine whether Adpgk$_{Mut}$/TLR3/CD40 vaccination-induced

283 CX3CR1+CD8+ T cells contain tumor-specific T cells other than Adpgk$_{Mut}$-specific T cells.
284 Nevertheless, this observation suggests the potential utility of CX3CR1 as a blood-based
285 predictive T-cell biomarker for other immunotherapies such as immune checkpoint inhibitor
286 therapy. Indeed, an increased frequency of PB CX3CR1+CD8+ T cells was observed in
287 patients who responded to immune checkpoint inhibitors (45, 53).

288 Our work and others have provided some insights into the theoretical advantages of
289 CX3CR1 as a circulating surrogate marker for vaccine efficacy. Vaccine-primed CX3CR1+CD8+
290 T cells expressed low levels of CD62L and CXCR3, trafficking receptors necessary for entry
291 across lymphoid organ HEV and the tumor microvasculature (16, 17), respectively, that may
292 have contributed to increase its frequency in PB. Furthermore, unlike other T-cell
293 proliferation, activation or co-stimulatory/inhibitory molecules transiently expressed after
294 activation, CX3CR1 is stably expressed on CD8+ T cells through unidirectional differentiation
295 from CX3CR1-CD8+ T cells during the effector phase (13-15).

296 Although the scope of our study is limited to CX3CR1, another future area of
297 investigation would be to compare the utility of CX3CR1 as a circulating surrogate marker for
298 vaccine efficacy with other molecules such as PD-1, which was reported to be expressed in
299 circulating neoantigen-specific CD8+ T cells (54). Notably, our study was limited by the use of a
300 transplantable non-orthotopic mouse tumor model with high mutational burden. Thus, the utility
301 of CX3CR1 as a circulating T-cell biomarker for vaccine therapy targeting endogenous tumor-
302 associated antigens or tumors with lower mutational burden remains uncertain. Further studies in
303 genetically engineered mouse models or mouse tumors harboring endogenous tumor-associated
304 antigen are warranted to better understand the overall utility of CX3CR1 in vaccine therapy.

305 Our *in vivo* depletion study revealed negligible contribution of CX3CR1+CD8+ T cells
306 elicited by AdpgkMut/TLR3/CD40 vaccination against established MC38 tumors, in line with a
307 previous study using a preclinical model of adoptive T cell therapy against B16 melanoma (15).
308 These findings are in parallel to the compelling evidence that terminally-differentiated effector
309 CD8+ T cells have less antitumor efficacy *in vivo* compared to less-differentiated T cells (55, 56),
310 but in contrast to previous studies demonstrating decreased antitumor immunity in CX3CR1-/-
311 mice or with the use of the CX3CR1 antagonist (33, 42-45). A possible explanation is that in
312 *Cd2-cre/Cx3cr1+/DTR* mice, DT administration does not affect monocytes, DCs, M-MDSCs and
313 TAMs that may express CX3CR1 (46, 47) and negatively regulate antitumor immunity.
314 Another possibility is that CX3CR1/CX3CL1 pathway might not play a significant role in an
315 MC38 tumor model, and trafficking of CX3CR1+CD8+ T cells to the TME is not efficient in the
316 setting of their decreased CXCR3 expression (16). Previous preclinical studies using mouse and
317 xenograft tumor models revealed that augmenting CX3CR1/CX3CL1 axis enhances T
318 cell/NK-cell mediated antitumor efficacy (42, 57-59). Therefore, the role of CX3CR1+CD8+ T
319 cells in antitumor reactivity against solid malignancies might be context-dependent, and remains
320 to be elucidated.

321 In summary, our study revealed cDC1-mediated potent antitumor efficacy of neoantigen
322 vaccine with dual TLR3/CD40 stimulation, identified a correlation between antitumor response
323 and the frequency of antigen-specific PB CX3CR1+CD8+ T cells, and provided the mechanistic
324 insight into the generation of CX3CR1+CD8+ T cells. These data suggest the maximal
325 engagement of cDC1s with TLR3/CD40 stimulation for the development of more effective
326 neoantigen vaccine therapy, and the potential implications of CX3CR1 as a circulating T-cell
327 predictive biomarker for response in future clinical studies.

328 # Materials and Methods

329 **Mice**

330 Female C57BL/6 mice were purchased from the Jackson Laboratory. CD40$_{-/-}$ mice
331 (B6.129S2-*Cd40lg*$_{tm1Imx}$/J), CD80/86$_{-/-}$ mice (B6.129S4-*Cd80*$_{tm1Shr}$ *Cd86*$_{tm2Shr}$/J), and Basic
332 leucine zipper transcription factor ATF-like 3 (Batf3)$_{-/-}$ mice (B6.129S(C)-*Batf3*$_{tm1Kmm}$/J), CD2-
333 Cre mice (C57BL/6-Tg(CD2-cre)1Lov/J) (48), and CX3CR1-DTR mice (B6N.129P2-
334 Cx3cr1$_{tm3(DTR)Litt}$/J) (49) on C57BL/6 background were purchased from the Jackson Laboratory,
335 and bred in-house (Roswell Park Comprehensive Cancer Center). CD70$_{-/-}$ mice on C57BL/6
336 background have been previously described (60). For inducible *Cd2-cre/Cx3cr1*$_{+/DTR}$ mice, we
337 crossed CD2-Cre mice with CX3CR1-DTR mice to generate *Cd2-cre/Cx3cr1*$_{+/DTR}$ mice,
338 allowing induction of DTR in CX3CR1$_{+}$ CD8$_{+}$ T cells. For depletion of CX3CR1$_{+}$ CD8$_{+}$ T
339 cells, diphtheria toxin (Sigma) (250 ng/dose/mouse) was administered intraperitoneally (i.p.)
340 every day starting from 1 day before neoantigen vaccination. All mice were 7 to 12 weeks old
341 at the beginning of each experiment, and were maintained under specific pathogen-free
342 conditions at the Roswell Park animal facility according to approved institutional guidelines.

343

344 **Cells**

345 The murine B16F10 melanoma cell line was purchased from ATCC. The MC38 murine
346 colon adenocarcinoma cell line was gift from Dr. Weiping Zou (University of Michigan).
347 B16F10 and MC38 cells were maintained in RPMI (Gibco) supplemented with 10% FBS
348 (Sigma), 1% NEAA (Gibco), 2 mM GlutaMAX-1 (Gibco), 100 U/ml penicillin-streptomycin
349 (Gibco), and 55 μM 2-mercaptoethanol (Gibco). Cells were authenticated by morphology,

350 phenotype and growth, and routinely screened for *Mycoplasma*, and were maintained at 37°C in
351 a humidified 5% CO_2 atmosphere.
352
353 ***In vivo* vaccination and cancer immunotherapy studies**
354 Female C57BL/6 mice were injected s.c. with 5-8 × 10^5 MC38 cells into the right flank.
355 Mice were treated s.c. with 100 µg soluble $Adpgk_{Mut}$ (ASMTNMELM) or AH1 (SPSYVYHQF)
356 peptide (GenScript) with 50 µg poly(I:C) (InvivoGen) and 50 µg agonistic CD40 Ab (BioXCell,
357 clone FGK45) in 100 µl of PBS into the left flank twice 1 week apart. PB, spleen and tumors
358 were harvested for immune monitoring 1 week after the 2nd vaccination. Tumor volumes were
359 calculated by determining the length of short (l) and long (L) diameters (volume = $l^2 \times L/2$).
360 Experimental end points were reached when tumors exceeded 20 mm in diameter or when mice
361 became moribund and showed signs of lateral recumbency, cachexia, lack of response to noxious
362 stimuli, or observable weight loss.
363
364 **Generation of bone marrow chimeras**
365 To generate bone marrow chimeras, C57BL/6 mice were irradiated with 500 cGy
366 followed by a second dose of 550 cGy 3 hours apart. To obtain donor bone marrow, femurs and
367 tibiae were harvested and the bone marrow was flushed out. For Batf3$^{-/-}$/WT, Batf3$^{-/-}$/CD40$^{-/-}$,
368 Batf3$^{-/-}$/CD80/86$^{-/-}$, and Batf3$^{-/-}$/CD70$^{-/-}$ mixed bone marrow chimeras, 5 × 10^6 bone marrow
369 cells of a 1:1 mixture were injected to irradiated C57BL/6 WT mice. After 8-12 weeks,
370 recipients were used for the experiments.
371
372 **Flow cytometry and intracellular granzyme, TNF-α and IFN-γ assay**

373 Fluorochrome-conjugated antibodies are shown in Table S1. DAPI, LIVE/DEAD Fixable
374 Aqua (Thermo Fisher Scientific) staining cells were excluded from analysis. For tetramer
375 staining, PE-labeled MHC class I (H-2D$_b$) specific for mouse Adpgk$_{Mut}$ 299-307
376 (ASMTNMELM)(18) was kindly provided by the NIH Tetramer Core Facility. Detection of
377 intracellular cytokines, GZMA, IFN-γ and TNF-α was performed as described before (15, 61).
378 For intracellular staining of IFN-γ and TNF-α, splenocytes and tumor-infiltrating cells were
379 cocultured with 1 μmol/L of Adpgk$_{Mut}$ or AH1 peptide in the presence of Brefeldin A (BD
380 Biosciences) for 5h *in vitro*. Samples were analyzed using an LSR II or an LSRFortessa (BD
381 Biosciences) with FlowJo software (TreeStar).
382
383 **Statistical Analysis**
384 Continuous measures were compared between two groups using two-tailed t-tests
385 (unpaired and paired) and between multiple groups using one-way ANOVA, with Tukey
386 adjusted post-hoc tests. Survival outcomes were compared using the log-rank test (Mantel-Cox
387 method). Correlations were assessed using the Pearson and Spearman correlation coefficients.
388 Analyses were performed in GraphPad Prism 8.02 (GraphPad Software) and SAS v9.4 (Cary,
389 NC) at a significance level of 0.05.
390
391
392

Competing interests

The authors declare no conflict of interest.

Author contributions

T.Y. contributed development of methodology, acquisition of data, analysis and interpretation of data, writing, review, and revision of the manuscript.

T.H, contributed development of methodology, acquisition of data, analysis and interpretation of data, review, and revision of the manuscript.

T.O. contributed acquisition of data, analysis and interpretation of data, review, and revision of the manuscript.

K.A. contributed analysis and interpretation of data, review, and revision of the manuscript.

X.C. provided CD70$^{-/-}$ mice, review, and revision of the manuscript.

F.I. contributed conception and design, development of methodology, acquisition of data, analysis and interpretation of data, writing, review, and finalizing the manuscript.

Acknowledgments

We acknowledge the NIH Tetramer Core Facility (contract HHSN272201300006C) for provision of MHC class I tetramers, Dr. Weiping Zou (University of Michigan, Ann Arbor, Michigan) for MC38 cells, Dr. James J. Moon (University of Michigan, Ann Arbor, Michigan) and Dr. Toshihiro Yokoi (Roswell Park) for technical assistance, and Dr. Suzanne M. Hess and Ms. Judith Epstein for administrative assistance. This work was supported by National Cancer Institute (NCI) grant P30CA016056 involving the use of Roswell Park's Flow and Image

415 Cytometry, Genomic Shared, and Biostatistics & Statistical Genomics Resources. This work was
416 supported by Roswell Park Alliance Foundation and NCI/ K08CA197966 (F. Ito), Uehara
417 Memorial Foundation (T. Oba), and Astellas Foundation for Research on Metabolic Disorders
418 and the Nakatomi Foundation (T. Yamauchi).
419
420

421 # References

422 1. Butterfield LH. Cancer vaccines. *BMJ (Clinical research ed).* 2015;350:h988.
423 2. Melero I, Gaudernack G, Gerritsen W, Huber C, Parmiani G, Scholl S, et al. Therapeutic
424 vaccines for cancer: an overview of clinical trials. *Nature reviews Clinical oncology.*
425 2014;11(9):509-24.
426 3. Schumacher TN, and Schreiber RD. Neoantigens in cancer immunotherapy. *Science.*
427 2015;348(6230):69-74.
428 4. Sahin U, Derhovanessian E, Miller M, Kloke BP, Simon P, Lower M, et al. Personalized
429 RNA mutanome vaccines mobilize poly-specific therapeutic immunity against cancer.
430 *Nature.* 2017;547(7662):222-6.
431 5. Keskin DB, Anandappa AJ, Sun J, Tirosh I, Mathewson ND, Li S, et al. Neoantigen
432 vaccine generates intratumoral T cell responses in phase Ib glioblastoma trial. *Nature.*
433 2019;565(7738):234-9.
434 6. Ott PA, Hu Z, Keskin DB, Shukla SA, Sun J, Bozym DJ, et al. An immunogenic personal
435 neoantigen vaccine for patients with melanoma. *Nature.* 2017;547(7662):217-21.
436 7. Hilf N, Kuttruff-Coqui S, Frenzel K, Bukur V, Stevanović S, Gouttefangeas C, et al.
437 Actively personalized vaccination trial for newly diagnosed glioblastoma. *Nature.*
438 2019;565(7738):240-5.
439 8. Fang Y, Mo F, Shou J, Wang H, Luo K, Zhang S, et al. A pan-cancer clinical study of
440 personalized neoantigen vaccine monotherapy in treating patients with various types of
441 advanced solid tumors. *Clin Cancer Res.* 2020.
442 9. Chen F, Zou Z, Du J, Su S, Shao J, Meng F, et al. Neoantigen identification strategies
443 enable personalized immunotherapy in refractory solid tumors. *J Clin Invest.*
444 2019;129(5):2056-70.
445 10. Fridman WH, Pages F, Sautes-Fridman C, and Galon J. The immune contexture in
446 human tumours: impact on clinical outcome. *Nat Rev Cancer.* 2012;12(4):298-306.
447 11. Galon J, Costes A, Sanchez-Cabo F, Kirilovsky A, Mlecnik B, Lagorce-Pages C, et al.
448 Type, density, and location of immune cells within human colorectal tumors predict
449 clinical outcome. *Science.* 2006;313(5795):1960-4.
450 12. Rosenberg SA, Sherry RM, Morton KE, Scharfman WJ, Yang JC, Topalian SL, et al.
451 Tumor progression can occur despite the induction of very high levels of self/tumor
452 antigen-specific CD8+ T cells in patients with melanoma. *J Immunol.* 2005;175(9):6169-
453 76.
454 13. Gordon CL, Lee LN, Swadling L, Hutchings C, Zinser M, Highton AJ, et al. Induction
455 and Maintenance of CX3CR1-Intermediate Peripheral Memory CD8(+) T Cells by
456 Persistent Viruses and Vaccines. *Cell Rep.* 2018;23(3):768-82.
457 14. Gerlach C, Moseman EA, Loughhead SM, Alvarez D, Zwijnenburg AJ, Waanders L, et
458 al. The Chemokine Receptor CX3CR1 Defines Three Antigen-Experienced CD8 T Cell
459 Subsets with Distinct Roles in Immune Surveillance and Homeostasis. *Immunity.*
460 2016;45(6):1270-84.
461 15. Yamauchi T, Hoki T, Oba T, Saito H, Attwood K, Sabel MS, et al. CX3CR1-CD8+ T
462 cells are critical in antitumor efficacy, but functionally suppressed in the tumor
463 microenvironment. *JCI insight.* 2020;5(8):e133920.

464 16. Mikucki ME, Fisher DT, Matsuzaki J, Skitzki JJ, Gaulin NB, Muhitch JB, et al. Non-
465 redundant requirement for CXCR3 signalling during tumoricidal T-cell trafficking across
466 tumour vascular checkpoints. *Nature communications.* 2015;6:7458.
467 17. von Andrian UH, and Mempel TR. Homing and cellular traffic in lymph nodes. *Nat Rev*
468 *Immunol.* 2003;3(11):867-78.
469 18. Yadav M, Jhunjhunwala S, Phung QT, Lupardus P, Tanguay J, Bumbaca S, et al.
470 Predicting immunogenic tumour mutations by combining mass spectrometry and exome
471 sequencing. *Nature.* 2014;515(7528):572-6.
472 19. Nimanong S, Ostroumov D, Wingerath J, Knocke S, Woller N, Gurlevik E, et al. CD40
473 Signaling Drives Potent Cellular Immune Responses in Heterologous Cancer
474 Vaccinations. *Cancer research.* 2017;77(8):1918-26.
475 20. Scarlett UK, Cubillos-Ruiz JR, Nesbeth YC, Martinez DG, Engle X, Gewirtz AT, et al.
476 In situ stimulation of CD40 and Toll-like receptor 3 transforms ovarian cancer-infiltrating
477 dendritic cells from immunosuppressive to immunostimulatory cells. *Cancer research.*
478 2009;69(18):7329-37.
479 21. Khalil DN, Suek N, Campesato LF, Budhu S, Redmond D, Samstein RM, et al. In situ
480 vaccination with defined factors overcomes T cell exhaustion in distant tumors. *J Clin*
481 *Invest.* 2019;129(8):3435-47.
482 22. Ahonen CL, Doxsee CL, McGurran SM, Riter TR, Wade WF, Barth RJ, et al. Combined
483 TLR and CD40 triggering induces potent CD8+ T cell expansion with variable
484 dependence on type I IFN. *The Journal of experimental medicine.* 2004;199(6):775-84.
485 23. Carbone DP, Ciernik IF, Kelley MJ, Smith MC, Nadaf S, Kavanaugh D, et al.
486 Immunization with mutant p53- and K-ras-derived peptides in cancer patients: immune
487 response and clinical outcome. *J Clin Oncol.* 2005;23(22):5099-107.
488 24. Kirkwood JM, Lee S, Moschos SJ, Albertini MR, Michalak JC, Sander C, et al.
489 Immunogenicity and antitumor effects of vaccination with peptide vaccine+/-
490 granulocyte-monocyte colony-stimulating factor and/or IFN-alpha2b in advanced
491 metastatic melanoma: Eastern Cooperative Oncology Group Phase II Trial E1696. *Clin*
492 *Cancer Res.* 2009;15(4):1443-51.
493 25. Dillon PM, Olson WC, Czarkowski A, Petroni GR, Smolkin M, Grosh WW, et al. A
494 melanoma helper peptide vaccine increases Th1 cytokine production by leukocytes in
495 peripheral blood and immunized lymph nodes. *Journal for immunotherapy of cancer.*
496 2014;2:23.
497 26. Sanchez-Paulete AR, Cueto FJ, Martinez-Lopez M, Labiano S, Morales-Kastresana A,
498 Rodriguez-Ruiz ME, et al. Cancer Immunotherapy with Immunomodulatory Anti-CD137
499 and Anti-PD-1 Monoclonal Antibodies Requires BATF3-Dependent Dendritic Cells.
500 *Cancer Discov.* 2016;6(1):71-9.
501 27. Bennett SR, Carbone FR, Karamalis F, Flavell RA, Miller JF, and Heath WR. Help for
502 cytotoxic-T-cell responses is mediated by CD40 signalling. *Nature.* 1998;393(6684):478-
503 80.
504 28. Ridge JP, Di Rosa F, and Matzinger P. A conditioned dendritic cell can be a temporal
505 bridge between a CD4+ T-helper and a T-killer cell. *Nature.* 1998;393(6684):474.
506 29. Schoenberger SP, Toes RE, van der Voort EI, Offringa R, and Melief CJ. T-cell help for
507 cytotoxic T lymphocytes is mediated by CD40-CD40L interactions. *Nature.*
508 1998;393(6684):480-3.

509 30. Cho HI, and Celis E. Optimized peptide vaccines eliciting extensive CD8 T-cell
510 responses with therapeutic antitumor effects. *Cancer research.* 2009;69(23):9012-9.
511 31. Bullock TN. TNF-receptor superfamily agonists as molecular adjuvants for cancer
512 vaccines. *Curr Opin Immunol.* 2017;47:70-7.
513 32. Zander R, Schauder D, Xin G, Nguyen C, Wu X, Zajac A, et al. CD4(+) T Cell Help Is
514 Required for the Formation of a Cytolytic CD8(+) T Cell Subset that Protects against
515 Chronic Infection and Cancer. *Immunity.* 2019;51(6):1028-42.e4.
516 33. Ahrends T, Spanjaard A, Pilzecker B, Babala N, Bovens A, Xiao Y, et al. CD4(+) T Cell
517 Help Confers a Cytotoxic T Cell Effector Program Including Coinhibitory Receptor
518 Downregulation and Increased Tissue Invasiveness. *Immunity.* 2017;47(5):848-61.e5.
519 34. Fuertes MB, Kacha AK, Kline J, Woo SR, Kranz DM, Murphy KM, et al. Host type I
520 IFN signals are required for antitumor CD8+ T cell responses through CD8{alpha}+
521 dendritic cells. *The Journal of experimental medicine.* 2011;208(10):2005-16.
522 35. Hildner K, Edelson BT, Purtha WE, Diamond M, Matsushita H, Kohyama M, et al. Batf3
523 deficiency reveals a critical role for CD8alpha+ dendritic cells in cytotoxic T cell
524 immunity. *Science.* 2008;322(5904):1097-100.
525 36. Broz ML, Binnewies M, Boldajipour B, Nelson AE, Pollack JL, Erle DJ, et al. Dissecting
526 the tumor myeloid compartment reveals rare activating antigen-presenting cells critical
527 for T cell immunity. *Cancer Cell.* 2014;26(5):638-52.
528 37. Salmon H, Idoyaga J, Rahman A, Leboeuf M, Remark R, Jordan S, et al. Expansion and
529 Activation of CD103(+) Dendritic Cell Progenitors at the Tumor Site Enhances Tumor
530 Responses to Therapeutic PD-L1 and BRAF Inhibition. *Immunity.* 2016;44(4):924-38.
531 38. Rech AJ, Dada H, Kotzin JJ, Henao-Mejia J, Minn AJ, Twyman-Saint Victor C, et al.
532 Radiotherapy and CD40 Activation Separately Augment Immunity to Checkpoint
533 Blockade in Cancer. *Cancer research.* 2018;78(15):4282-91.
534 39. Morrison AH, Diamond MS, Hay CA, Byrne KT, and Vonderheide RH. Sufficiency of
535 CD40 activation and immune checkpoint blockade for T cell priming and tumor
536 immunity. *Proc Natl Acad Sci U S A.* 2020;117(14):8022-31.
537 40. Edelson BT, Kc W, Juang R, Kohyama M, Benoit LA, Klekotka PA, et al. Peripheral
538 CD103+ dendritic cells form a unified subset developmentally related to CD8alpha+
539 conventional dendritic cells. *The Journal of experimental medicine.* 2010;207(4):823-36.
540 41. Bak SP, Barnkob MS, Bai A, Higham EM, Wittrup KD, and Chen J. Differential
541 requirement for CD70 and CD80/CD86 in dendritic cell-mediated activation of tumor-
542 tolerized CD8 T cells. *J Immunol.* 2012;189(4):1708-16.
543 42. Xin H, Kikuchi T, Andarini S, Ohkouchi S, Suzuki T, Nukiwa T, et al. Antitumor
544 immune response by CX3CL1 fractalkine gene transfer depends on both NK and T cells.
545 *Eur J Immunol.* 2005;35(5):1371-80.
546 43. Zeng Y, Huebener N, Fest S, Weixler S, Schroeder U, Gaedicke G, et al. Fractalkine
547 (CX3CL1)- and interleukin-2-enriched neuroblastoma microenvironment induces
548 eradication of metastases mediated by T cells and natural killer cells. *Cancer research.*
549 2007;67(5):2331-8.
550 44. Yu YR, Fong AM, Combadiere C, Gao JL, Murphy PM, and Patel DD. Defective
551 antitumor responses in CX3CR1-deficient mice. *Int J Cancer.* 2007;121(2):316-22.
552 45. Yan Y, Cao S, Liu X, Harrington SM, Bindeman WE, Adjei AA, et al. CX3CR1
553 identifies PD-1 therapy-responsive CD8+ T cells that withstand chemotherapy during
554 cancer chemoimmunotherapy. *JCI insight.* 2018;3(8):e97828.

555 46. Nishimura M, Umehara H, Nakayama T, Yoneda O, Hieshima K, Kakizaki M, et al. Dual
556 functions of fractalkine/CX3C ligand 1 in trafficking of perforin+/granzyme B+ cytotoxic
557 effector lymphocytes that are defined by CX3CR1 expression. *J Immunol.*
558 2002;168(12):6173-80.
559 47. Bronte V, Brandau S, Chen SH, Colombo MP, Frey AB, Greten TF, et al.
560 Recommendations for myeloid-derived suppressor cell nomenclature and characterization
561 standards. *Nature communications.* 2016;7:12150.
562 48. Vacchio MS, Wang L, Bouladoux N, Carpenter AC, Xiong Y, Williams LC, et al. A
563 ThPOK-LRF transcriptional node maintains the integrity and effector potential of post-
564 thymic CD4+ T cells. *Nat Immunol.* 2014;15(10):947-56.
565 49. Diehl GE, Longman RS, Zhang JX, Breart B, Galan C, Cuesta A, et al. Microbiota
566 restricts trafficking of bacteria to mesenteric lymph nodes by CX(3)CR1(hi) cells. *Nature.*
567 2013;494(7435):116-20.
568 50. Elgueta R, Benson MJ, de Vries VC, Wasiuk A, Guo Y, and Noelle RJ. Molecular
569 mechanism and function of CD40/CD40L engagement in the immune system. *Immunol*
570 *Rev.* 2009;229(1):152-72.
571 51. Borst J, Ahrends T, Babala N, Melief CJM, and Kastenmuller W. CD4(+) T cell help in
572 cancer immunology and immunotherapy. *Nat Rev Immunol.* 2018;18(10):635-47.
573 52. Tian Y, Cox MA, Kahan SM, Ingram JT, Bakshi RK, and Zajac AJ. A Context-
574 Dependent Role for IL-21 in Modulating the Differentiation, Distribution, and
575 Abundance of Effector and Memory CD8 T Cell Subsets. *J Immunol.* 2016;196(5):2153-
576 66.
577 53. Wallin JJ, Bendell JC, Funke R, Sznol M, Korski K, Jones S, et al. Atezolizumab in
578 combination with bevacizumab enhances antigen-specific T-cell migration in metastatic
579 renal cell carcinoma. *Nature communications.* 2016;7:12624.
580 54. Gros A, Parkhurst MR, Tran E, Pasetto A, Robbins PF, Ilyas S, et al. Prospective
581 identification of neoantigen-specific lymphocytes in the peripheral blood of melanoma
582 patients. *Nat Med.* 2016;22(4):433-8.
583 55. Gattinoni L, Klebanoff CA, Palmer DC, Wrzesinski C, Kerstann K, Yu Z, et al.
584 Acquisition of full effector function in vitro paradoxically impairs the in vivo antitumor
585 efficacy of adoptively transferred CD8+ T cells. *J Clin Invest.* 2005;115(6):1616-26.
586 56. Restifo NP, Dudley ME, and Rosenberg SA. Adoptive immunotherapy for cancer:
587 harnessing the T cell response. *Nat Rev Immunol.* 2012;12(4):269-81.
588 57. Guo J, Zhang M, Wang B, Yuan Z, Guo Z, Chen T, et al. Fractalkine transgene induces
589 T-cell-dependent antitumor immunity through chemoattraction and activation of dendritic
590 cells. *Int J Cancer.* 2003;103(2):212-20.
591 58. Kee JY, Arita Y, Shinohara K, Ohashi Y, Sakurai H, Saiki I, et al. Antitumor immune
592 activity by chemokine CX3CL1 in an orthotopic implantation of lung cancer model in
593 vivo. *Molecular and clinical oncology.* 2013;1(1):35-40.
594 59. Siddiqui I, Erreni M, van Brakel M, Debets R, and Allavena P. Enhanced recruitment of
595 genetically modified CX3CR1-positive human T cells into Fractalkine/CX3CL1
596 expressing tumors: importance of the chemokine gradient. *Journal for immunotherapy of*
597 *cancer.* 2016;4:21.
598 60. O'Neill RE, Du W, Mohammadpour H, Alqassim E, Qiu J, Chen G, et al. T Cell-Derived
599 CD70 Delivers an Immune Checkpoint Function in Inflammatory T Cell Responses. *J*
600 *Immunol.* 2017;199(10):3700-10.

601 61. Saito H, Okita K, Chang AE, and Ito F. Adoptive Transfer of CD8+ T Cells Generated
602 from Induced Pluripotent Stem Cells Triggers Regressions of Large Tumors Along with
603 Immunological Memory. *Cancer research.* 2016;76(12):3473-83.

604

Figure 1

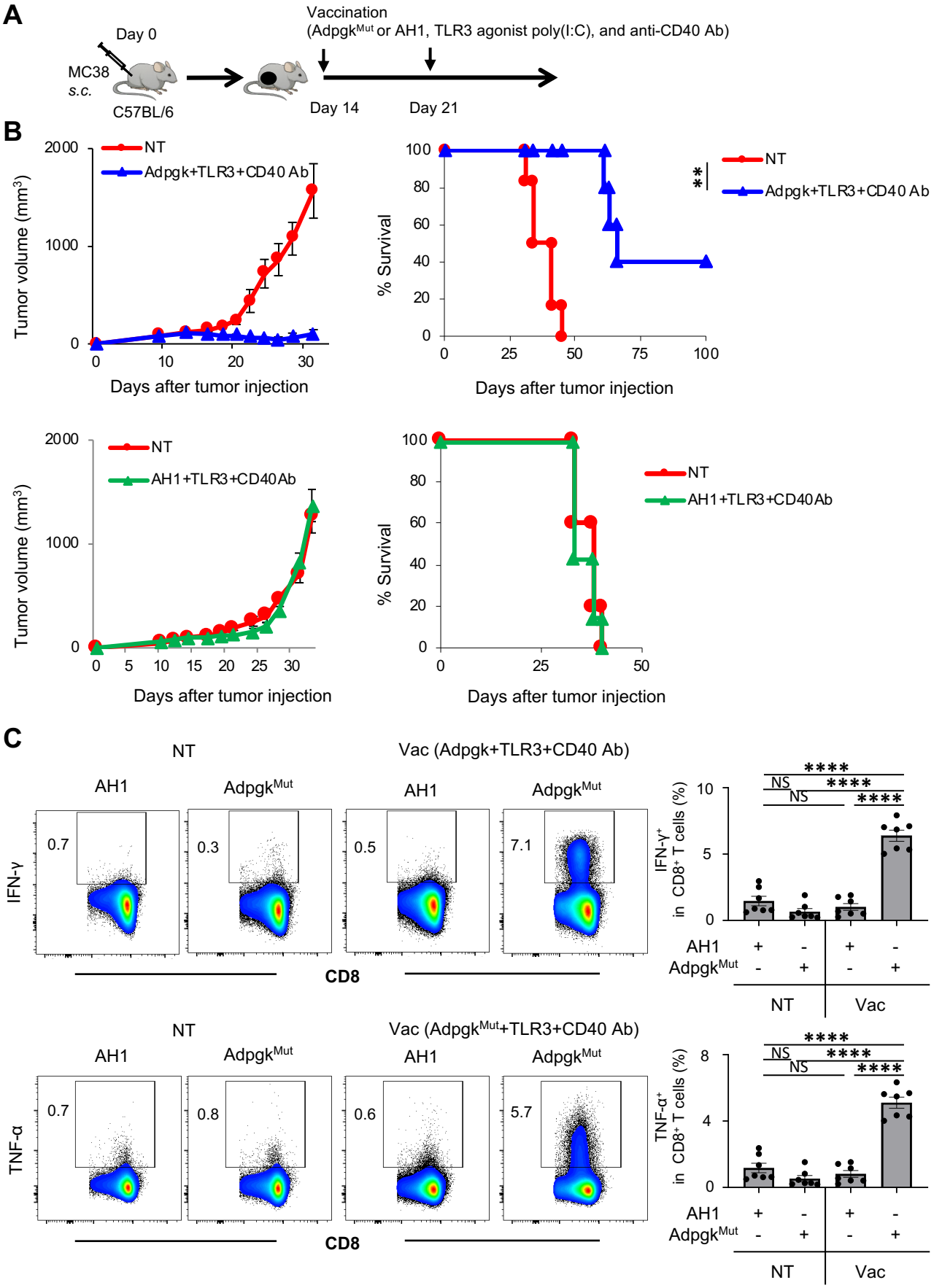
A
Day 0
MC38
s.c.
C57BL/6
Vaccination
(Adpgk^Mut or AH1, TLR3 agonist poly(I:C), and anti-CD40 Ab)
Day 14
Day 21
B
NT
Adpgk+TLR3+CD40 Ab
Tumor volume (mm³)
Days after tumor injection
% Survival
**
AH1+TLR3+CD40Ab
C
NT
Vac (Adpgk+TLR3+CD40 Ab)
AH1
Adpgk^Mut
IFN-γ
0.7
0.3
0.5
7.1
CD8
IFN-γ⁺ in CD8⁺ T cells (%)
NS
****
Vac (Adpgk^Mut+TLR3+CD40 Ab)
TNF-α
0.8
0.6
5.7
TNF-α⁺ in CD8⁺ T cells (%)

Figure 1. Vaccination with neoantigen and TLR3/CD40 agonists elicits potent antigen-specific antitumor efficacy.

(A) Experimental scheme for evaluation of neoantigen/TLR3/CD40 agonists vaccination (Vac) in an MC38 tumor model (refer Materials and Methods for details).

(B) Tumor growth and survival curves in MC38 tumor-bearing C57BL/6 mice treated with PBS (NT: non-treatment) or $Adpgk_{Mut}$/TLR3/CD40 agonists vaccination (upper) (n = 6 mice per group) and PBS (NT) or AH1/TLR3/CD40 agonists vaccination (lower) (n = 5-7 mice per group).

(C) Left shows representative FACS plots showing CD8 and IFN-γ (upper) or TNF-α (lower) expression gated with $CD8_+$ T cells in splenocytes of MC38-tumor bearing mice 1 week after second PBS injection (NT) or $Adpgk_{Mut}$/TLR3/CD40 agonists vaccination. Splenocytes were co-cultured with $Adpgk_{Mut}$ or AH1 peptide in the presence of Brefeldin A for 5 hrs before intracellular staining. Numbers denote percentage of IFN-γ_+ or TNF-α_+ cells. Right panel shows the frequency of the IFN-γ_+ or TNF-α_+ cells in $CD8_+$ T cells in each group (n = 7 mice per group).

NS not significant, ****$P < 0.0001$ by log-rank (Mantel-Cox) test (B) and one-way ANOVA with Tukey's multiple comparisons (C). Mean ± SEM.

Figure 2

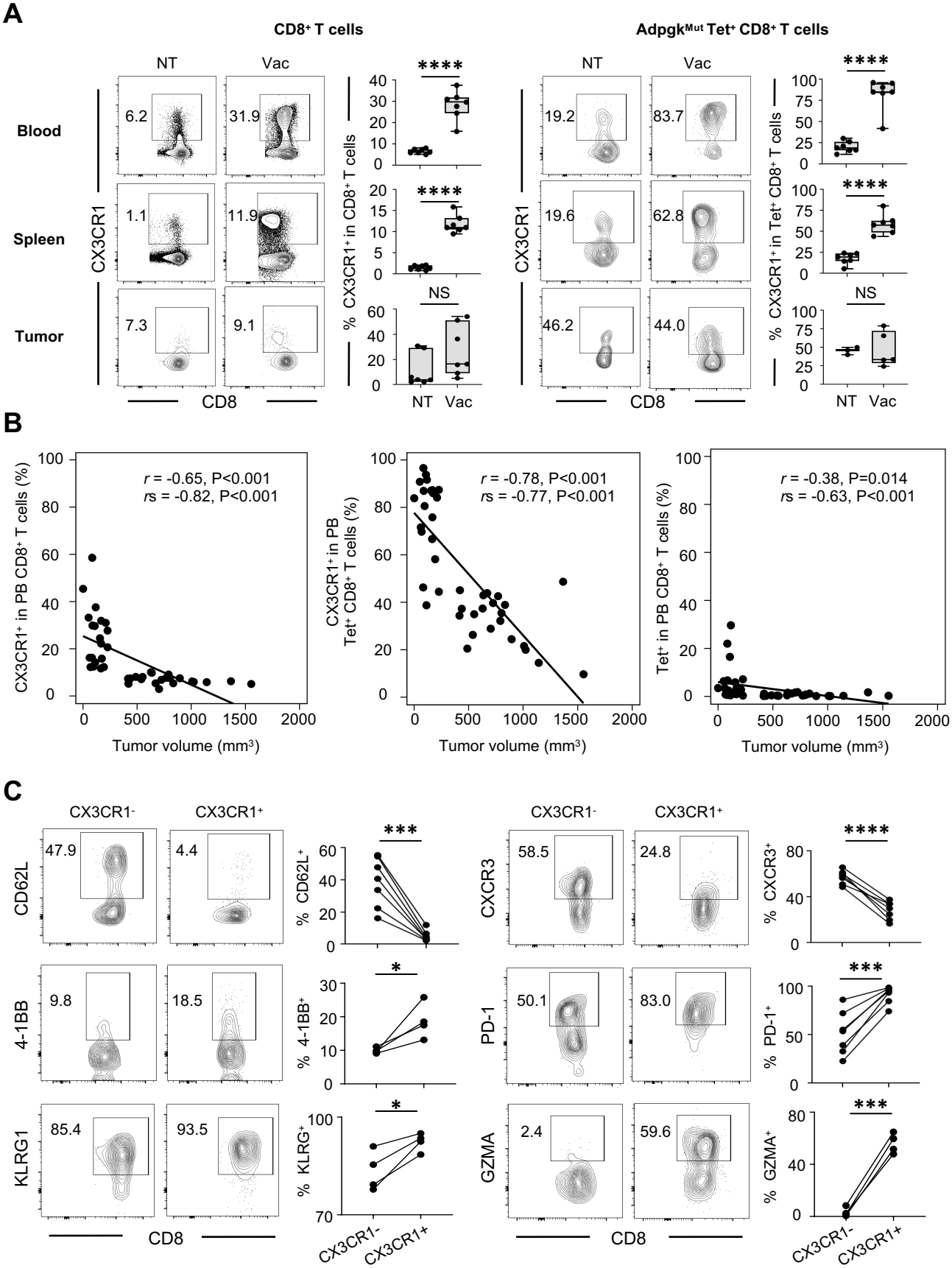
A
CD8+ T cells
AdpgkMut Tet+ CD8+ T cells
NT
Vac
Blood
Spleen
Tumor
CX3CR1
CD8
6.2
31.9
1.1
11.9
7.3
9.1
19.2
83.7
19.6
62.8
46.2
44.0
% CX3CR1+ in CD8+ T cells
% CX3CR1+ in Tet+ CD8+ T cells
****
NS
B
r = -0.65, P<0.001
rs = -0.82, P<0.001
CX3CR1+ in PB CD8+ T cells (%)
r = -0.78, P<0.001
rs = -0.77, P<0.001
CX3CR1+ in PB Tet+ CD8+ T cells (%)
r = -0.38, P=0.014
rs = -0.63, P<0.001
Tet+ in PB CD8+ T cells (%)
Tumor volume (mm3)
C
CX3CR1-
CX3CR1+
CD62L
4-1BB
KLRG1
CXCR3
PD-1
GZMA
47.9
4.4
9.8
18.5
85.4
93.5
58.5
24.8
50.1
83.0
2.4
59.6
% CD62L+
% 4-1BB+
% KLRG+
% CXCR3+
% PD-1+
% GZMA+
***
*
****

Figure 2. Effective neoantigen/TLR3/CD40 stimulations correlate with generation of antigen-specific effector CX3CR1$_+$CD8$_+$ T cells.

(A) Representative FACS plots showing CX3CR1 expression in CD8$_+$ (left) or Adpgk$_{Mut}$ tetramer (Tet)$_+$CD8$_+$ T cells (right) in peripheral blood (PB) (upper), spleen (middle) and tumors (lower) from MC38-tumor bearing mice 1 week after second Adpgk$_{Mut}$/TLR3/CD40 agonists vaccination (Vac). Numbers denote percentage of CX3CR1-positive cells. Frequency of CX3CR1-positive cells from the CD8$_+$ or Tet$_+$CD8$_+$ T cells is shown in the right panels (n = 3-7 mice per group). Data shown are representative of three independent experiments.

(B) Scatter plot of the frequency of PB CX3CR1$_+$CD8$_+$ (left), CX3CR1$_+$Tet$_+$CD8$_+$ T cells (middle), and Tet$_+$CD8$_+$ T cells against tumor volume in untreated and treated mice 1 week after second Adpgk$_{Mut}$/TLR3/CD40 agonists vaccination. Correlation is shown using Pearson correlation (r) and Spearman correlation coefficients (r_s). Data shown are representative of two independent experiments.

(C) Representative FACS plots of CX3CR1$_-$ (left) or CX3CR1$_+$ (right) cells gated with Tet$_+$CD8$_+$ T cells in PB of MC38-tumor bearing mice 1 week after second Adpgk$_{Mut}$/TLR3/CD40 agonists vaccination. Numbers denote percentage of each marker-positive cells. Frequency of marker-positive cells from the CX3CR1$_-$ or CX3CR1$_+$ subset is shown in the right panels for each marker (n = 4-7 mice per group). Data shown are representative of two independent experiments. NS: not significant, *$P < 0.05$, ***$P < 0.001$, ****$P < 0.0001$ by unpaired (A) and paired two-tailed t-test (C). Mean ± SEM.

Figure 3

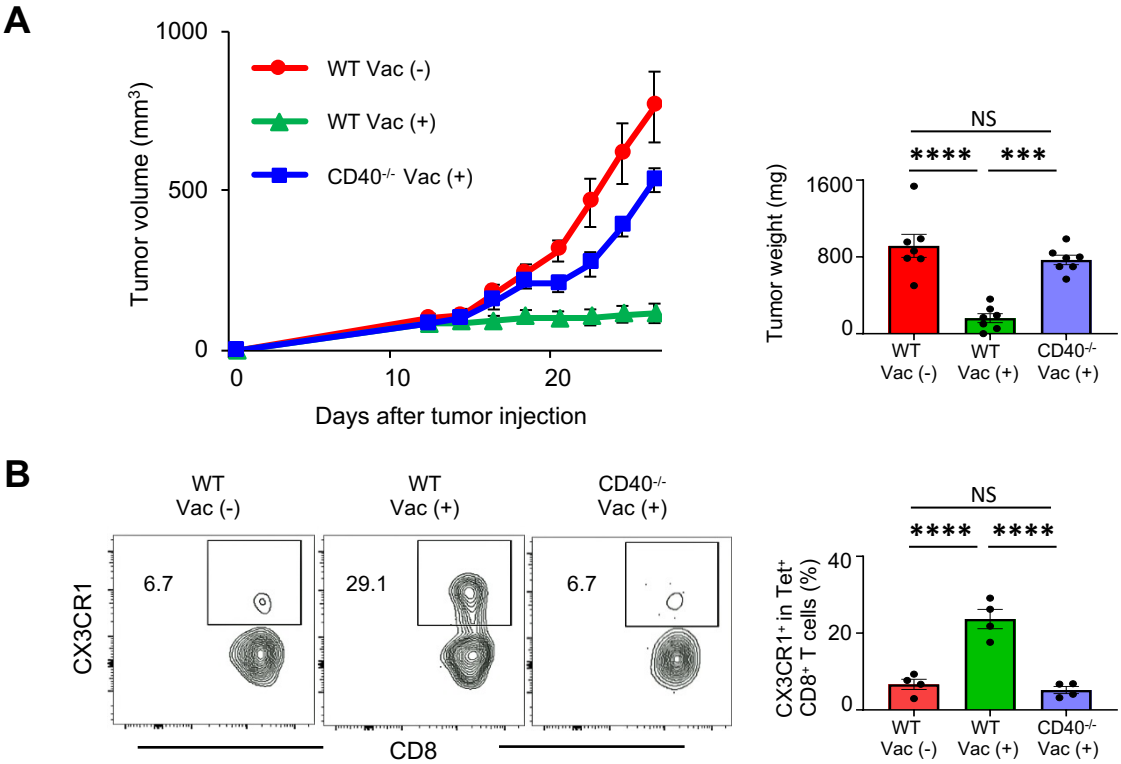
A
1000
500
0
Tumor volume (mm3)
WT Vac (-)
WT Vac (+)
CD40-/- Vac (+)
0
10
20
Days after tumor injection
NS
****
***
1600
800
0
Tumor weight (mg)
WT Vac (-)
WT Vac (+)
CD40-/- Vac (+)
B
WT Vac (-)
WT Vac (+)
CD40-/- Vac (+)
CX3CR1
6.7
29.1
6.7
CD8
NS
****
****
40
20
0
CX3CR1+ in Tet+ CD8+ T cells (%)
WT Vac (-)
WT Vac (+)
CD40-/- Vac (+)

Figure 3. CD40-dependent generation of antigen-specific CX3CR1$_{+}$CD8$_{+}$ T-cell subsets upon neoantigen/TLR3/CD40 agonists vaccination.

(A) Left shows tumor volume curves in MC38 tumor-bearing wild type C57BL/6 mice (WT) or CD40$_{-/-}$ mice treated with or without Adpgk$_{Mut}$/TLR3/CD40 agonists vaccination (Vac) (n = 7 mice per group). Right shows tumor weight. Tumors were harvested 1 week after second vaccination (Vac).

(B) Left shows representative FACS plots showing CD8 and CX3CR1 expression gated with Adpgk$_{Mut}$ Tet$_{+}$CD8$_{+}$ T cells in peripheral blood (PB) of MC38-tumor bearing WT or CD40 $_{-/-}$ mice treated with or without Vac. Numbers denote percentage of the CX3CR1$_{+}$ subset. Right shows the frequency of the CX3CR1$_{+}$ subset in each group (n = 4 mice per group). PB was harvested 1 week after second Vac. Data shown are representative of two independent experiments. NS: not significant, ***P <0.001, ****P <0.0001 by one-way ANOVA with Tukey's multiple comparisons. Mean ± SEM.

Figure 4

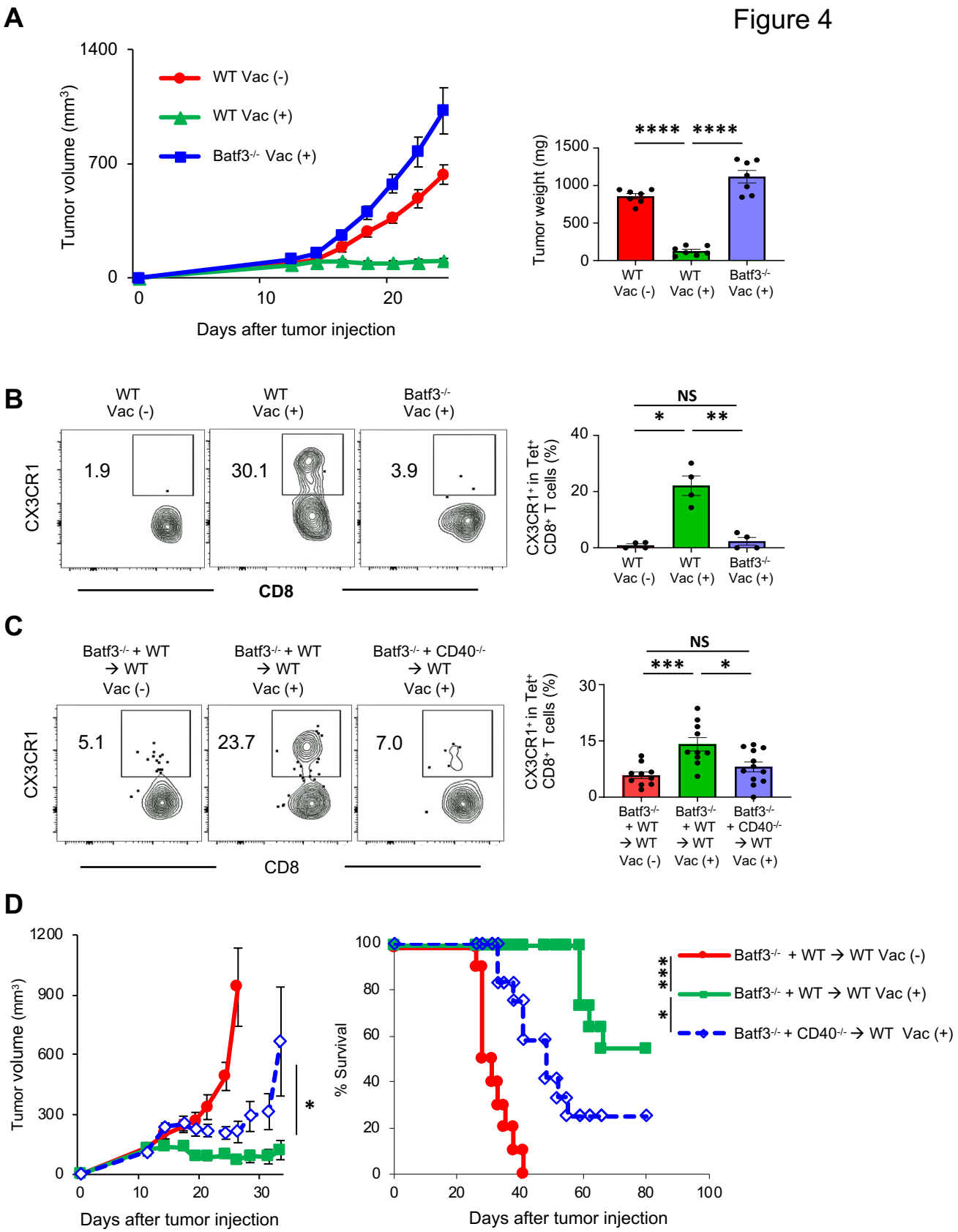
A
Tumor volume (mm³)
1400
700
0
WT Vac (-)
WT Vac (+)
Batf3-/- Vac (+)
0
10
20
Days after tumor injection
Tumor weight (mg)
1500
1000
500
0
****
****
WT Vac (-)
WT Vac (+)
Batf3-/- Vac (+)
B
WT Vac (-)
WT Vac (+)
Batf3-/- Vac (+)
CX3CR1
1.9
30.1
3.9
CD8
CX3CR1+ in Tet+ CD8+ T cells (%)
40
20
0
NS
*
**
WT Vac (-)
WT Vac (+)
Batf3-/- Vac (+)
C
Batf3-/- + WT → WT Vac (-)
Batf3-/- + WT → WT Vac (+)
Batf3-/- + CD40-/- → WT Vac (+)
CX3CR1
5.1
23.7
7.0
CD8
CX3CR1+ in Tet+ CD8+ T cells (%)
30
15
0
NS
***
*
Batf3-/- + WT → WT Vac (-)
Batf3-/- + WT → WT Vac (+)
Batf3-/- + CD40-/- → WT Vac (+)
D
Tumor volume (mm³)
1200
900
600
300
0
*
0
10
20
30
Days after tumor injection
% Survival
100
80
60
40
20
0
0
20
40
60
80
100
Days after tumor injection
***
*
Batf3-/- + WT → WT Vac (-)
Batf3-/- + WT → WT Vac (+)
Batf3-/- + CD40-/- → WT Vac (+)

Figure 4. Critical roles of CD40 signaling in cDC1s for antitumor efficacy of neoantigen/TLR3/CD40 agonists vaccination and generation of antigen-specific CX3CR1$_{+}$CD8$_{+}$ T cells.

(A) Left shows tumor volume curves in MC38 tumor-bearing wild type C57BL/6 mice (WT) or Batf3$_{-/-}$ mice treated with or without Adpgk$_{Mut}$/TLR3/CD40 agonists vaccination (Vac) (n = 7 mice per group). Tumors were harvested 1 week after second Vac, and tumor weight (mg) is shown in the right panel.

(B) Left shows representative FACS plots showing CD8 and CX3CR1 expression gated with PB Adpgk$_{Mut}$ Tet$_{+}$CD8$_{+}$ T cells in MC38 tumor-bearing WT or Batf3 $_{-/-}$ mice treated with or without Vac. Numbers denote percentage of the CX3CR1$_{+}$ subset. Right shows the frequency of the CX3CR1$_{+}$ subset in each group (n = 4 mice per group).

(C) Left shows representative FACS plots showing CD8 and CX3CR1 expression gated with Adpgk$_{Mut}$ Tet$_{+}$ CD8$_{+}$ T cells in PB of MC38-tumor bearing bone marrow chimera mice (Batf3$_{-/-}$ and WT→WT or Batf3$_{-/-}$ and CD40$_{-/-}$→WT mice) treated with or without Vac. PB was harvested 1 week after second Vac (B and C). Data shown are representative of two independent experiments (A, B and C).

(D) Tumor growth and survival curves in MC38 tumor-bearing mixed bone marrow chimera mice (Batf3$_{-/-}$ and WT→WT or Batf3$_{-/-}$ and CD40$_{-/-}$→WT mice) treated with or without Vac (n = 10-11 mice per group). Data shown are pooled from two independent experiments. $*P < 0.05$, $**P < 0.01$, $***P < 0.001$, $****P < 0.0001$ by one-way ANOVA with Tukey's multiple comparisons (A, B and C), Mann-Whitney *U* test (D for tumor volume), or log-rank (Mantel-Cox) test (D for survival). Mean ± SEM.

Figure 5

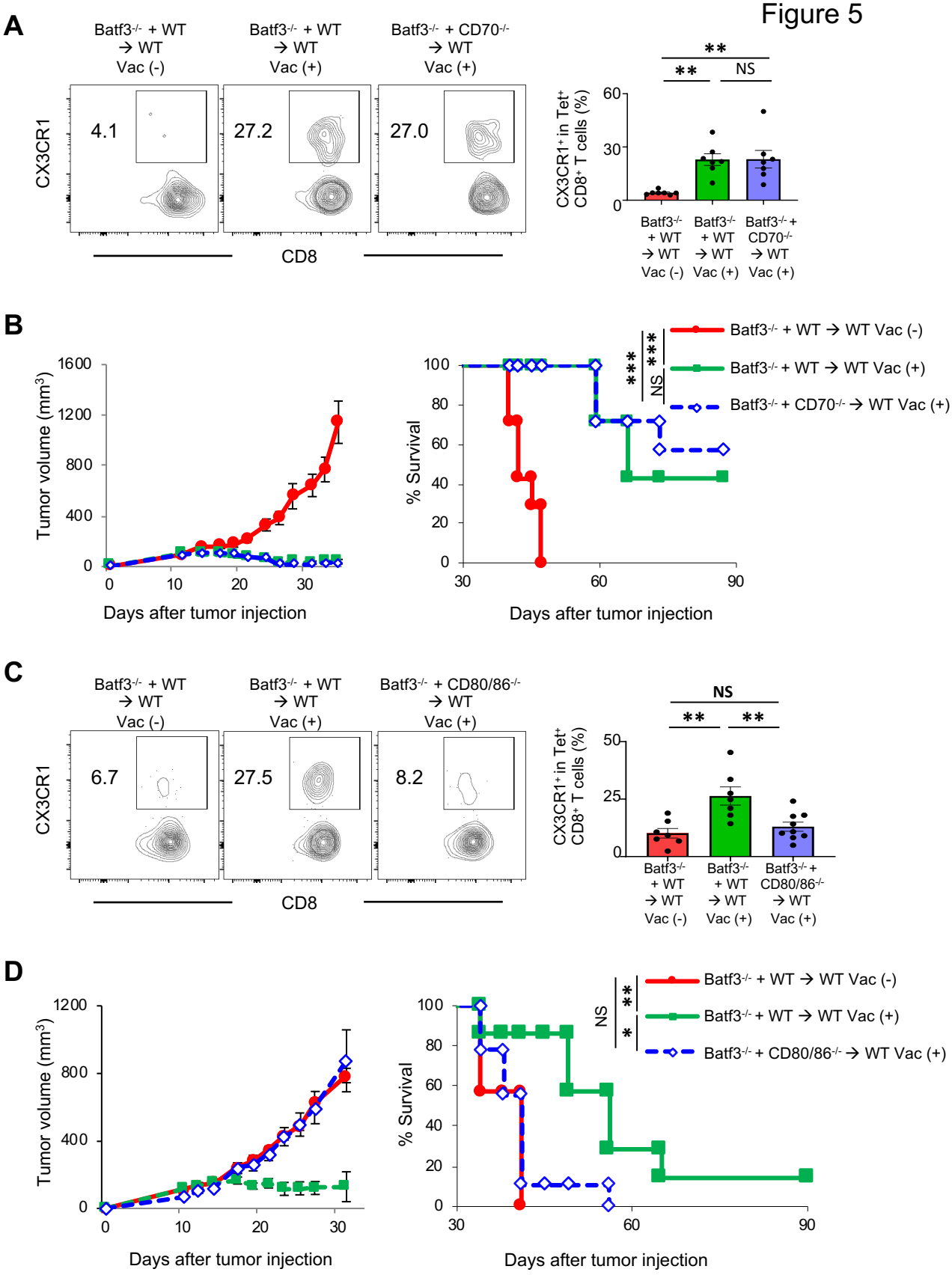
A
Batf3-/- + WT → WT Vac (-)
Batf3-/- + WT → WT Vac (+)
Batf3-/- + CD70-/- → WT Vac (+)
CX3CR1
4.1
27.2
27.0
CD8
CX3CR1+ in Tet+ CD8+ T cells (%)
**
**
NS
B
Tumor volume (mm3)
Days after tumor injection
% Survival
Batf3-/- + WT → WT Vac (-)
Batf3-/- + WT → WT Vac (+)
Batf3-/- + CD70-/- → WT Vac (+)
***
***
NS
C
Batf3-/- + WT → WT Vac (-)
Batf3-/- + WT → WT Vac (+)
Batf3-/- + CD80/86-/- → WT Vac (+)
CX3CR1
6.7
27.5
8.2
CD8
CX3CR1+ in Tet+ CD8+ T cells (%)
NS
**
**
D
Tumor volume (mm3)
Days after tumor injection
% Survival
Batf3-/- + WT → WT Vac (-)
Batf3-/- + WT → WT Vac (+)
Batf3-/- + CD80/86-/- → WT Vac (+)
NS
**
*

Figure 5. Roles of CD80/86 and CD70 signaling in cDC1s for antitumor efficacy of neoantigen/TLR3/CD40 agonists vaccination and generation of antigen-specific CX3CR1$_{+}$CD8$_{+}$ T cells.

(A) Left shows representative FACS plots showing CD8 and CX3CR1 expression gated with Adpgk$_{Mut}$ Tet$_{+}$ CD8$_{+}$ T cells in PB of MC38-tumor bearing bone marrow chimera mice (Batf3$_{-/-}$ and WT→WT or Batf3$_{-/-}$ and CD70$_{-/-}$→WT mice) treated with or without Adpgk$_{Mut}$/TLR3/CD40 agonists vaccination (Vac) Right shows the frequency of the CX3CR1$_{+}$Tet$_{+}$CD8$_{+}$ T cells in each group (n = 7 mice per group).

(B) Tumor growth and survival curves of MC38 tumor-bearing mixed bone marrow chimera mice in different treatment groups as indicated. (n = 7 mice per group)

(C) Left shows representative FACS plots showing CD8 and CX3CR1 expression gated with Adpgk$_{Mut}$ Tet$_{+}$ CD8$_{+}$ T cells in PB of MC38-tumor bearing bone marrow chimera mice (Batf3$_{-/-}$ and WT→WT or Batf3$_{-/-}$ and CD80/86$_{-/-}$→WT mice) treated with or without Vac (n = 7-9 mice per group).

(D) Tumor growth and survival curves of MC38 tumor-bearing mixed bone marrow chimera mice in different treatment groups as indicated (n = 7-9 mice per group).

PB was harvested 1 week after second Vac (A and C). Data shown are representative from two or three independent experiments. NS not significant, *P <0.05, **P <0.01, ***P <0.001 by one-way ANOVA with Tukey's multiple comparisons (A, C) or log-rank (Mantel-Cox) test (B, D). Mean ± SEM.

Figure 6

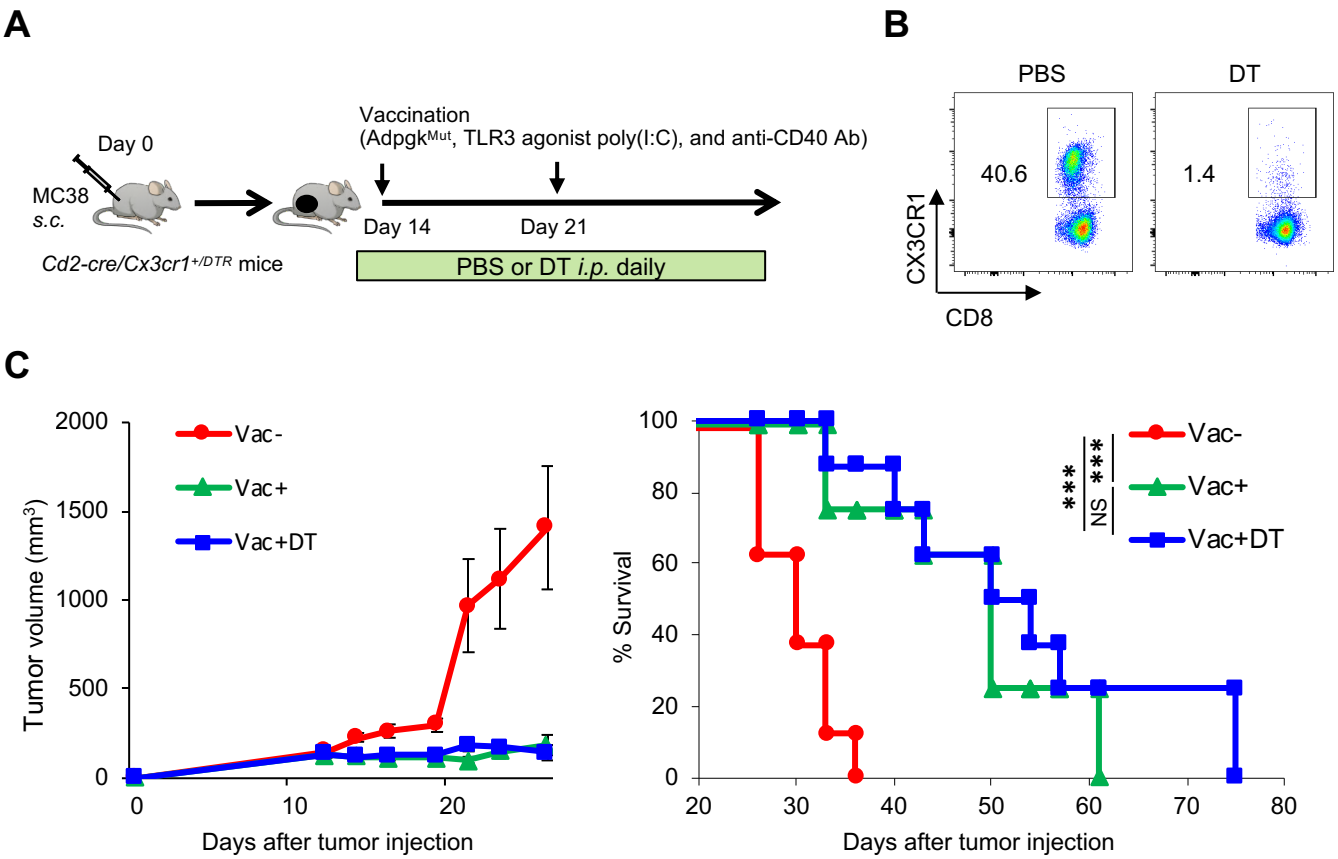
A
Day 0
MC38
s.c.
Cd2-cre/Cx3cr1+/DTR mice
Vaccination
(AdpgkMut, TLR3 agonist poly(I:C), and anti-CD40 Ab)
Day 14
Day 21
PBS or DT i.p. daily
B
PBS
DT
40.6
1.4
CX3CR1
CD8
C
Vac-
Vac+
Vac+DT
Tumor volume (mm3)
Days after tumor injection
% Survival
***
***
NS

Figure 6. *In vivo* antitumor efficacy of antigen-specific CX3CR1$_+$CD8$_+$ T cells elicited by neoantigen/TLR3/CD40 agonists vaccination.

(A) Schematic illustration showing evaluation of *in vivo* antitumor efficacy of the CX3CR1$_+$ subset using MC38 tumor-bearing *Cd2-cre/Cx3cr1$_{+/DTR}$* mice treated with Adpgk$_{Mut}$/TLR3/CD40 agonists vaccination (Vac) followed by diphtheria toxin (DT) administration. DT (250 ng) was injected intraperitoneally every day from day 13.

(B) Representative FACS plots showing selective depletion of CX3CR1$_+$ subset in PB upon DT injection in *Cd2-cre/Cx3cr1$_{+/DTR}$* mice treated with Vac. Expression of CX3CR1 in CD8$_+$ T cells in peripheral blood of mice treated with PBS or DT are shown. Numbers denote percentage of the CX3CR1$_+$ subset.

(C) Tumor growth and survival curves of MC38 tumor-bearing *Cd2-cre/Cx3cr1$_{+/DTR}$* mice in different treatment groups. ($n \geq 7$ mice per group). Data shown are representative of two independent experiments.

Data shown are representative from two independent experiments. ***$P < 0.001$, ****$P < 0.0001$ by log-rank (Mantel-Cox) test (C) or paired two-tailed *t*-test (D). Mean ± SEM.

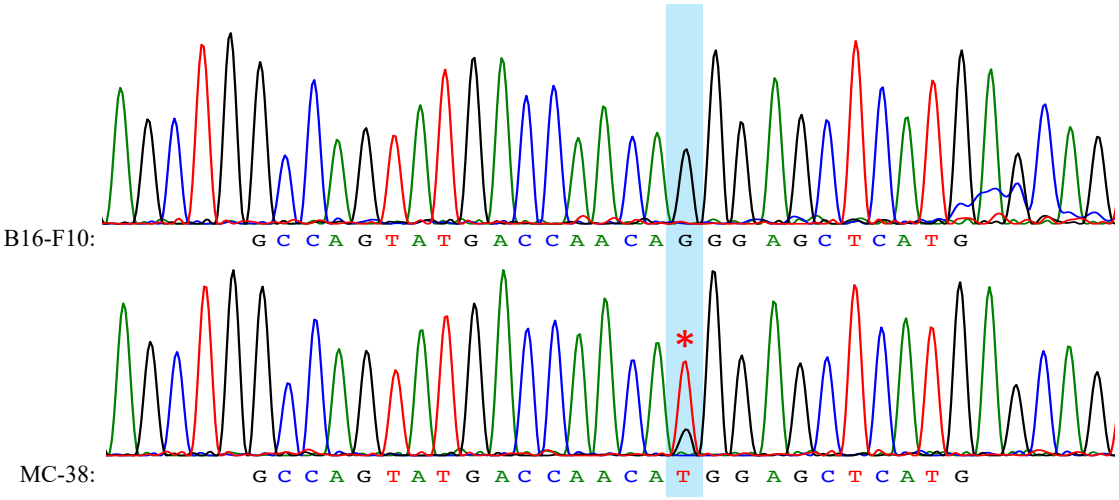

Supplementary Figure 1 cDNA sequencing of mutated Adpgk neoantigen in MC38 cells

Total RNA was extracted from MC38 cells (harboring mutated Adpgk) along with B16F10 cells (harboring wild type Adpgk), and subjected to cDNA synthesis for Sanger DNA sequencing. An asterisk indicates the mutation of G→T, resulting in arginine (R) to methionine (M) transformation on 304th amino acid sequences of Adpgk gene.

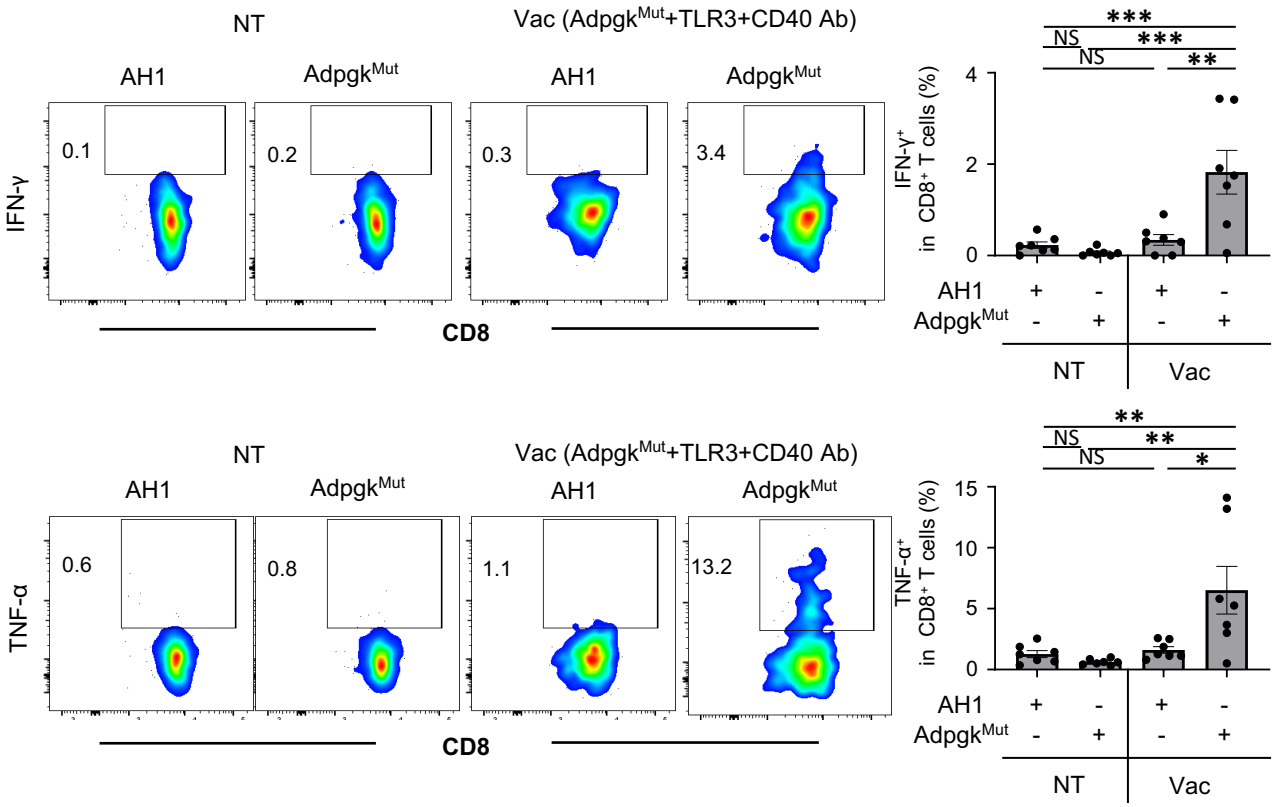

Supplementary Figure 2 Neoantigen/TLR3/CD40 vaccination facilitates neoantigen-specific CD8⁺ T cell infiltration into tumors

Left shows representative FACS plots showing CD8 and IFN-γ (upper) or TNF-α (lower) expression gated with CD8⁺ T cells in tumors of MC38-tumor bearing mice treated with PBS (NT) or neoantigen/TLR3/CD40 vaccinations. Tumor cells were co-cultured with AH1 or Adpgk peptide in the presence of blefeldin A for 5 hrs before intracellular staining. Numbers denote percentage of IFN-γ⁺ or TNF-α⁺ cells. Right panel shows the frequency of the IFN-γ⁺ cells in CD8⁺ T cells in each group (n = 7 mice per group). Data shown are representative from two or three independent experiments. NS not significant, $^{*}P < 0.05$, $^{**}P < 0.01$, $^{***}P < 0.001$ by one-way ANOVA with Tukey's multiple comparisons. Mean ± SEM.

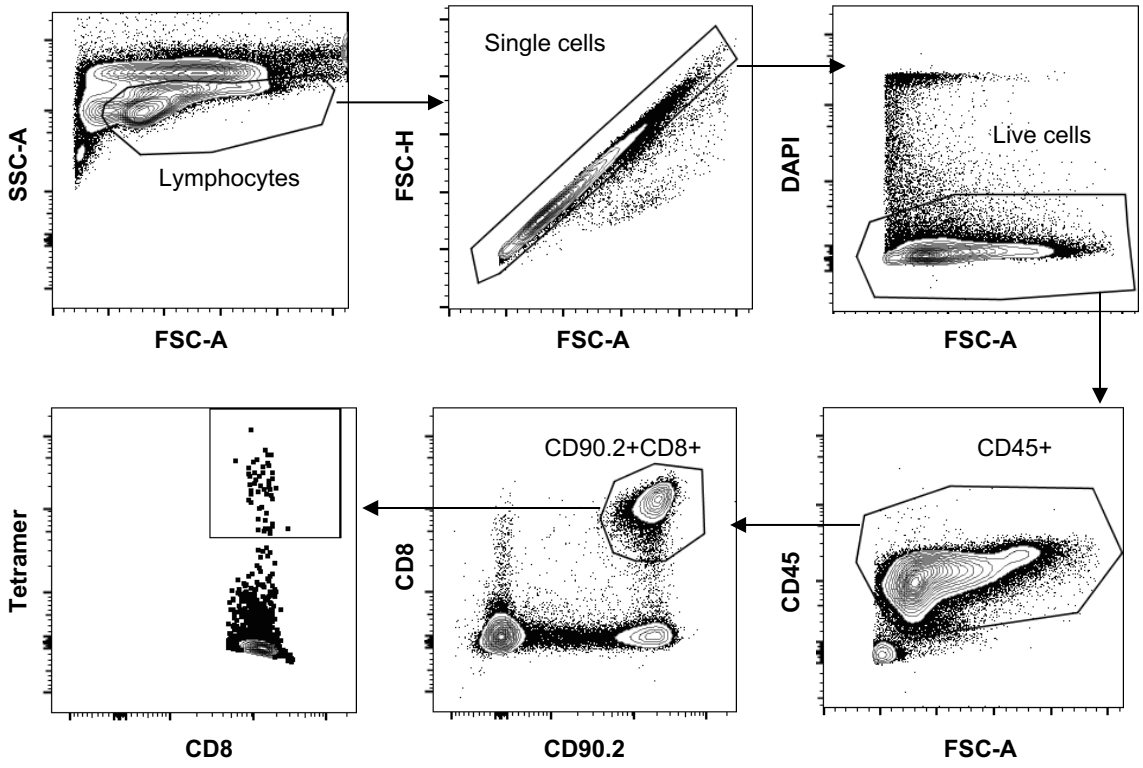

Supplementary Figure 3 Flow cytometry and gating of circulating Adpgk^{Mut} neoantigen-specific CD8^{+} T cells in MC38-tumor bearing mice. Representative of greater than 5 independent experiments.

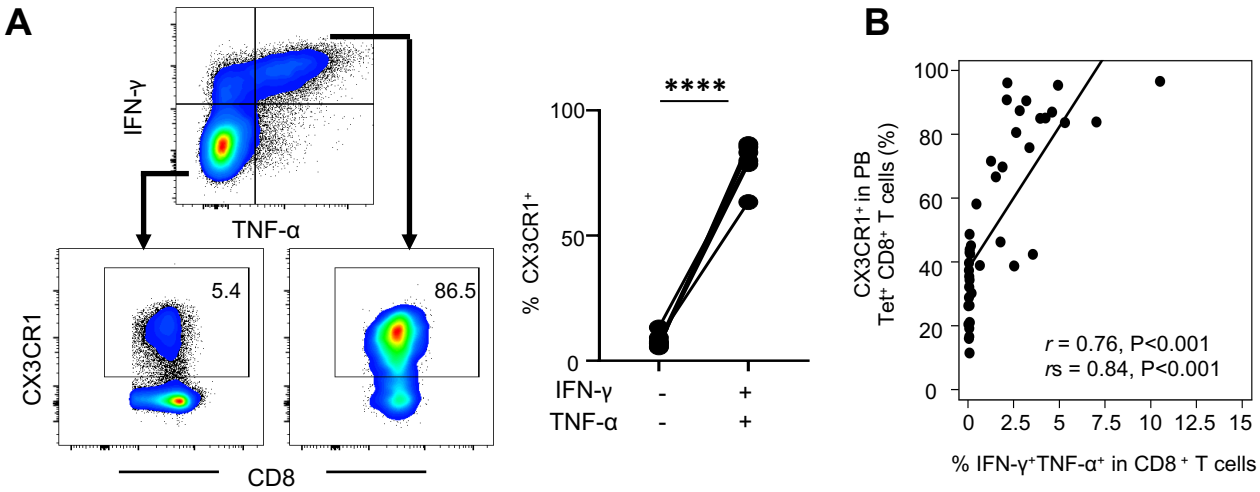

Supplementary Figure 4. High frequency of CX3CR1$^+$ subset in neoantigen/TLR3/CD40 vaccination-induced peripheral CD8$^+$ T cells that are capable of producing effector cytokines.

(A) Representative FACS plots showing IFN-γ and TNF-α expression gated with CD8$^+$ T cells in splenocytes of MC38-tumor bearing mice treated with Adpgk^{Mut}/TLR3/CD40 vaccinations. Lower panels show CX3CR1 expression in IFN-γ$^-$ TNF-α$^-$ cells (left) and IFN-γ$^+$ TNF-α$^+$ cells (right). Numbers denote percentage of CX3CR1$^+$ cells. Data shown are representative of three independent experiments. Frequency of CX3CR1 cells from the IFN-γ$^-$ TNF-α$^-$ or IFN-γ$^+$ TNF-α$^+$ subset is shown in the right panel (n = 7 mice per group). Spleens were harvested 1 week after second vaccination. ****$P < 0.0001$ by paired two-tailed *t*-test (A).
(B) Scatter plot of the frequency of IFN-γ$^+$TNF-α$^+$ cells against the frequency of Adpgk^{Mut} tetramer (Tet)$^+$ CX3CR1$^+$CD8$^+$ T cells in splenocytes. Correlation is shown using Pearson correlation (r) and Spearman correlation coefficients (r_s).
Data shown are representative of two independent experiments.

Table S1: Fluorochrome-conjugated antibodies used in flow cytometry

Antibody	Clone	Manufacturer
CD8	53-6.7	Biolegend
CD90.1	OX-7	BioLegend
CD90.2	53-2.1	BioLegend
CX3CR1	SA011F11	BioLegend
CD45	30-F11	BD Biosciences
CD62L	MEL-14	Biolegend
4-1BB	17B5	BioLegend
KLRG1	2F1	BD Biosciences
CXCR3	CXCR3-173	Biolegend
PD-1	29F.1A12	Biolegend
Granzyme A	GzA-3G8.5	Thermofisher
IFN-γ	XMG1.2	BD Biosciences
TNF-α	MP6-XT22	Biolegend